

**ECHAHID HAMMA LAKHDAR UNIVERSITY - EL-OUED**  
**Under the Supervision of the DGRSDT and in collaboration with the CRTI**  
**International Pluridisciplinary PhD Meeting (IPPM'20)**  
**23-26, 2020 1<sup>st</sup> Edition, February**  
**Theme: Renewable Energy**

**Evaluate the effect of changing climatic conditions on the optical and thermal performance of a linear solar collector**

Mokhtar Ghodbane<sup>1\*</sup>, Boussad Boumeddane<sup>1</sup>, Abderrahmane Khechekhouche<sup>2</sup>

<sup>1</sup>Mechanical Engineering Department, Faculty of Technology. Saad DAHLAB University, Blida 1, Algeria.

<sup>2</sup>El-Oued University, Algeria.

\*Email: [ghmokhtar39seminaire@gmail.com](mailto:ghmokhtar39seminaire@gmail.com)

### **Abstract**

One of the main axes adopted by the Algerian state is the work to develop renewable energy technologies, especially solar energy, in regions with a large abundance of solar radiation. Through this study, the optical and thermal behavior of a linear Fresnel solar reflector was studied. This technology has been used as a device to produce superheated steam. The energy balance equations were analyzed and then programmed on the Matlab to obtain the results. The finite differences method has been used to simplify and approximate equations. El-Oued's desert climate region was chosen for the study. Four different days of the year have been chosen for this study. The optical efficacy identified by this study has reached 53.60%, where the thermal efficiency is equal to 37.3%. The average values of overall coefficient of heat loss " $U_L$ , (W/m<sup>2</sup>.K)" was limited between 5.71837 (W/m<sup>2</sup>.K) and 5.98112 (W/m<sup>2</sup>.K). With regard to superheated steam, the temperature in December reached 500.9913 (K), where this is the lowest value recorded during the study. The results obtained are very encouraging to invest in electric plants that produce superheated steam by this linear collector.

**Keywords:** Solar energy; Linear Fresnel Reflector; Optical efficiencies; Thermal efficiencies; Superheated water steam.

### **1. Introduction**

The current global energy situation illustrates that most countries in the world are very dependent on fossil fuels (oil, gas and coal) to meet their needs. Hydrocarbons, the dominant energy source, cover 80% of global energy production. At this speed of exploration and exploitation, the situation of hydrocarbon reserves is extremely worrying and their environmental impact is very alarming {Ghodbane, 2017 #1;Ghodbane, 2016 #21}.

As an alternative to these concerns, the development and implementation of renewable energies is unavoidable. Unlimited and abundant energy resources exist and must be exploited; among these energies, we find solar energy, hydropower, wind power, geothermal energy, biomass energy and new hydrogen energy [1].

Solar energy is one of the most important types of renewable energies mentioned above. It can be used in many industrial and domestic fields. There are many techniques for using solar energy (linear concentrators, punctual concentrates, flat collectors, photovoltaic cells) [2-5].

Currently, solar concentrating technologies have the greatest potential for commercial exploitation of this energy source for power generation, given their profitability in terms of performance, and high yields can be achieved {Bellos, 2019 #20}.

What interests us in this study is the exploitation of one of the linear techniques of solar concentrators; this technique is the Linear Fresnel solar reflector (LFR). The French physicist Augustin-Jean FRESNEL (1788-1827) conceived this technology [6-8]. The work of Alessandro BATTAGLIA is the origin of the concentration technique by linear Fresnel reflector [6-8].

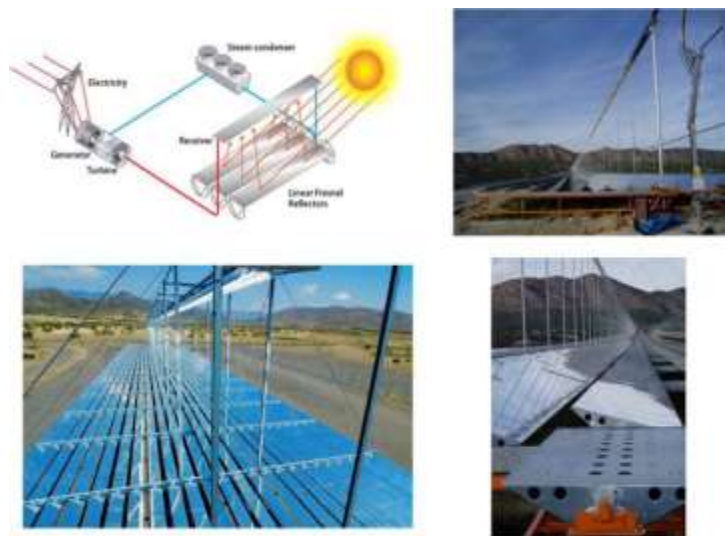


**Fig. 1.** Schematic and view of Fresnel solar power plants [9].

In this paper, we will present numerical simulation results for a linear Fresnel solar concentrator in El-Oued. The coordinates of the selected area for the completion of the solar power station in Algeria are: the latitude is 33.605084 North, the longitude is 6.799574,19 East and the altitude equals 62m. To conduct this study has been chosen four days, these days are 21/03/2018, 21/06/2018, 21/09/2018 and 21/12/2018.

The main objective of this study is to follow the optical and thermal behaviors of the linear Fresnel solar reflector in an Algerian region with a desert climate. These solar concentrators will allow us to produce superheated steam that will be used in power plants. The numerical solution was adopted in this study to analyze the equations of the energy balance. The study will also show the effect of climatic conditions on the efficacy of the device.

## 2. Energy balance equations

Performance modeling (optical and thermal) is based on the energy balances characterized by the differential equations of the three temperatures: TF (for the heat transfer fluid), TV (for the glass tube) and TA (for the absorber tube). These equations vary during the illumination time (t) for a length ( $\Delta X$ ) of the absorber. The finite difference method was used to analyze and approximate the energy balance equations.

The most important element in Fresnel-type linear concentration systems is the absorber tube in which the heat transfer fluid circulates inside. The absorber tube is often of copper covered with a suitable selective layer and surrounded by a glass tube, it is placed along the focal line of the Fresnel concentrator.

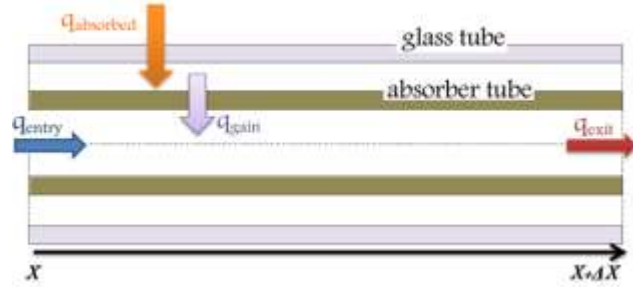


**Fig. 2.** Heat balance on a segment of LFR solar reflector.

The existing thermal exchanges for the Fresnel linear solar concentrator are between the three elements: the heat transfer fluid (HTF), the absorber tube and the glass cover. The incident direct solar radiation reflected by the Fresnel mirrors falls on the absorber tube, after passing through the glass tube. This incident solar energy absorbed by the absorber tube is not entirely transmitted to the heat transfer fluid, where a part is dissipated in the form of heat loss between the absorber tube and the glass tube, and another part is lost between the glass tube and the ambient air.

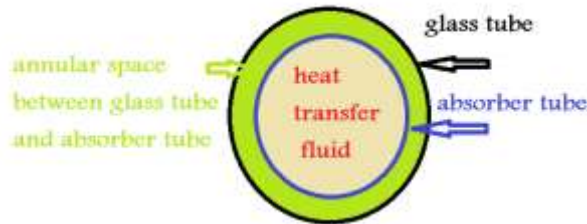


**Fig. 3.** Cross section of the absorber tube {Ghodbane, 2019 #6}.

### 2.1. Energy balance for the fluid

The energy balance for the heat transfer fluid flowing through the absorber tube is given by [10-12]:

$$\rho_F \cdot C_F \cdot A_{A,int} \cdot \frac{\partial T_F(X,t)}{\partial t} = q_{util} - \rho_F \cdot C_F \cdot Q_v \cdot \frac{\partial T_F(X,t)}{\partial X} \tag{1}$$

Where  $\rho_F$  is the heat transfer fluid density (kg.m<sup>-3</sup>);  $C_F$  is the specific heat of the heat transfer fluid (J.kg<sup>-1</sup>.k<sup>-1</sup>);  $A_{A,int}$  is the inner surface of the absorber tube (m<sup>2</sup>) ;  $Q_v$  is the volume flow rate of the heat transfer fluid in the absorber tube (m<sup>3</sup>.s);  $q_{util}$  is the quantity of heat exchanged by convection between the absorber tube and the heat transfer fluid (W).

The boundary and initial conditions of the equation (1) are [10-12]:

$$\begin{aligned} T_F(0,t) &= T_{F,\text{entry}}(t) = 413.15 \text{ K} \\ T_F(X,0) &= T_{F,\text{initial}}(X) = 413.15 \text{ K} \end{aligned} \quad (2)$$

All the thermo-physiques characteristics of heat transfer fluid are change with its temperature.

## 2.2. Energy balance for the absorber tube

The energy balance for the absorber tube is given the following equation [10-12].

$$\rho_A \cdot C_A \cdot A_A \cdot \frac{\partial T_A(X,t)}{\partial t} = q_{\text{absorbed}}(t) - q_{\text{exit}}(X,t) - q_{\text{gain}}(X,t) \quad (3)$$

With  $\rho A$  is the density of the absorber tube ( $\text{kg.m}^{-3}$ );  $C_A$  is the specific heat of the absorber tube ( $\text{J.kg}^{-1}.\text{k}^{-1}$ );  $A_A$  is the difference between the inner and the outer surface of the absorber tube ( $\text{m}^2$ );  $q_{\text{absorbed}}$  is the quantity of heat absorbed by the absorber tube (W);  $q_{\text{exit}}$  is the amount of heat from fluid when it came out of tube (W).

The initial conditions of the equation (3) are [10-12]:

$$T_A(X,0) = T_{A,\text{initial}}(0) = T_{\text{amb}}(0) \quad (4)$$

## 2.3. Energy balance of the glass tube

In the same way, the energy balance for the glass tube is given by [10-12] :

$$\rho_V \cdot C_V \cdot A_V \cdot \frac{\partial T_V(X,t)}{\partial t} = q_{\text{int}}(X,t) - q_{\text{ext}}(X,t) \quad (5)$$

Where  $\rho V$  is the density of the glass tube ( $\text{kg.m}^{-3}$ );  $C_V$  is the specific heat of glass ( $\text{J.kg}^{-1}.\text{k}^{-1}$ );  $A_V$  is the difference between the inner and the outer surface of the glass ( $\text{m}^2$ );  $q_{\text{int}}$  is the internal power (convection and radiation) between absorber and glass (W);  $q_{\text{ext}}$  is the external power (convection and radiation) between glass and the atmosphere (W).

Equation (6) shows the initial conditions of the equation (5) [10-12]:

$$T_V(X,0) = T_{V,\text{initial}}(0) = T_{\text{amb}}(0) \quad (6)$$

The thermal power emitted by the sun and received by the LFR solar reflector is given by [10-13]:

$$q_{\text{absorbed}} = \alpha \cdot \tau \cdot \rho_m \cdot \gamma \cdot S_e \cdot K_t(\theta_t) \cdot K_l(\theta_l) \cdot \text{DNI} \quad (7)$$

With  $S_e$  is the effective surface of LFR collector ( $\text{m}^2$ );  $\rho_m$  is the mirror reflectance factor;  $\alpha$  is the absorption coefficient of the absorber tube;  $\gamma$  is the interception factor,  $K_l(\theta_l)$  is the correction factor of the incidence

angle modified in the longitudinal plane;  $K_t(\theta_t)$  is the correction factor of the modified angle of incidence in the transverse plane and  $\tau$  is the transmission coefficient of the glass tube.

It can express the optical efficiency ( $\eta_{opt}$ ) of the concentrator by [10-12, 14].

$$\eta_{opt} = \alpha \cdot \tau \cdot \rho_m \cdot \gamma \cdot K_t(\theta_t) \cdot K_1(\theta_1) \quad (8)$$

The thermal efficiency ( $\eta_{th}$ ) is given by the equation (9) [10-12, 14]:

$$\eta_{th} = \eta_{opt} - \frac{U_L \cdot A_A \cdot (T_A - T_{amb})}{DNI \times S_e} \quad (9)$$

With  $U_L$  is the coefficient of heat loss ( $W/m^2.K$ ) and  $T_{amb}$  is the ambient temperature ( $K$ ).

#### 2.4. Heat loss coefficient

The coefficient of heat loss ( $U_L$ ) is expressed by [10-12]:

$$U_L = \left( \frac{1}{C_1 \left[ \frac{T_A - T_{amb}}{1+f} \right]^{\frac{1}{4}}} + \frac{D_{A,ext}}{D_{V,int} \times h_v} \right)^{-1} + \left( \frac{\sigma(T_A^2 + T_{amb}^2) \cdot (T_A + T_{amb})}{[A_1]^{-1} + [A_2]} \right) \quad (10)$$

With,

$$A_1 = \varepsilon_A - 0.04(1 - \varepsilon_A) \left( \frac{T_A}{450} \right) \quad (11)$$

$$A_2 = \left( \frac{D_{A,ext}}{D_{V,int}} \right) \left( \frac{1}{\varepsilon_V} - 1 \right) + \left( \frac{f}{\varepsilon_V} \right)$$

Where  $\varepsilon_A$  is the emissivity of the absorber tube;  $\varepsilon_V$  is the emissivity of the transparent glass envelope;  $\sigma$  is Stefan-Boltzmann constant ( $\sigma = 5.670 \times 10^{-8} W.m^{-2}.K^{-4}$ ).

The factor ( $f$ ) takes into account the wind loss coefficient, it is given by [10-12]:

$$f = D_{A,int}^{-0.4} (1.61 + 1.3 \varepsilon_A) h_v^{-0.9} \times \exp[0.00325(T_A - 273)] \quad (12)$$

With  $C_1$  is given by the following empirical expression [10-12]:

$$C_1 = \frac{1.45 + 0.96(\epsilon_A - 0.5)^2}{D_{A,ext} \left( \frac{1}{D_{A,ext}^{0.6}} + \frac{1}{D_{V,int}^{0.6}} \right)^{\frac{5}{4}}} \quad (13)$$

The term “ $h_v$ , (W/m<sup>2</sup>.K)” is the wind convection coefficient. according to McAdams (1954), it can be obtained by the following equation [15, 16]:

$$h_v = 5.7 + 3.8V \quad (14)$$

Where V is the speed of the wind, (m.s-1).

Therefore, there are three unknowns (TF, TA and TV). To resolve system reformulates of all relations, it will be adapted the following matrix form:

$$[\text{The coefficient matrix}] \times [\text{the vector of unknowns TF, TA and TV}] = [\text{vector of the second member}]$$

Where, the vector of the second member is not null.

Table (1) contains the engineering dimensions of the linear Fresnel solar reflector.

**Table 1.** Geometric dimensions of the lfr solar reflector.

Geometric Dimension	Value
Outside diameter of the absorber ( $D_{A,ext}$ )	0.070 m
Inner diameter of the absorber ( $D_{A,int}$ )	0.065 m
Outside diameter of the glass ( $D_{V,ext}$ )	0.115 m
Inner diameter of the glass ( $D_{V,int}$ )	0.109 m
Total Mirror of aperture area (L)	89.6 m
Total width of aperture area (l)	11.4643 m

Table (2) contains the Optical properties of the linear Fresnel solar reflector.

**Table 2.** Optical Characteristics Of The LFR Solar Reflector.

Parameter	Value
global average optical error ( $\sigma_{optique}$ )	03 mrad
Reflectance of mirror ( $\rho_m$ )	0.92
Transmissivity of the glass	0.945
Absorptivity of the absorber ( $\alpha$ )	0.94
Emissivity of the absorber tube ( $\epsilon_A$ )	0.12
Emissivity of the glass ( $\epsilon_V$ )	0.935

The numerical calculation method used is a means for determining performance (optical and thermal). Below, all the results of the numerical simulation were presented according to the variation of the climatic conditions for the four days selected to make this study.

### 3. Results and discussion

The main objective of this study is to produce superheated steam based on linear Fresnel solar concentrator in El-Oued area, Algeria. This superheated steam will allow the production of electricity at the power plants.

The energy balance equations were analyzed and rounded numerically, then programmed in MATLAB. The finite differences method has been used to simplify equations of energy.

#### 3.1. Climatic conditions

Figure (4) shows the evaluation of direct solar radiation “DNI, (W/m<sup>2</sup>)” according to time for the four days selected for study.

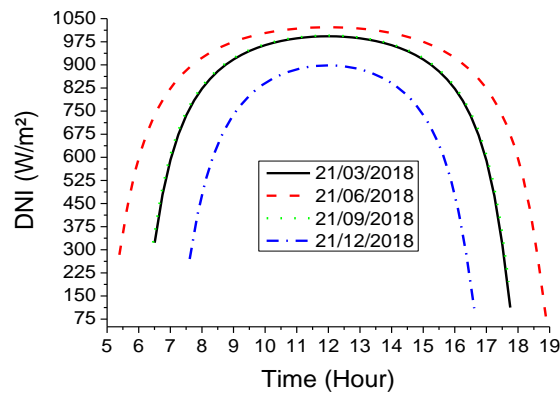


**Fig. 4.** Variation of the direct solar radiation.

It is noticeable that the change in direct solar radiation is very logical from sunrise to sunset. The maximum values of solar radiation for the four days starting March through December are as follows: 992.7994 (W/m<sup>2</sup>), 1022.031 (W/m<sup>2</sup>), 995.1583 (W/m<sup>2</sup>) and 898.2667 (W/m<sup>2</sup>). Figure (4) clearly shows the abundance of the selected area for conducting large quantities of direct solar radiation. This is a positive point for the use of solar energy by constructing solar power powers of various types.

#### 3.2. Efficiencies assessment of the LFR solar reflector

Generally, the linear Fresnel solar concentrator efficiency is the ratio between the useful heat transmitted from the absorber tube to the heat transfer fluid and the incident solar radiation.

As for optical efficiency “ $\eta_{opt}$ ”, it is related to the optical properties of linear Fresnel solar reflector components and relates to the rate of direct solar radiation access to the absorber tube. This ratio is evaluated using the intercept coefficient “ $\gamma$ ”. Figure (5) illustrates the optical efficiencies evaluation according to time for the four days selected for study.

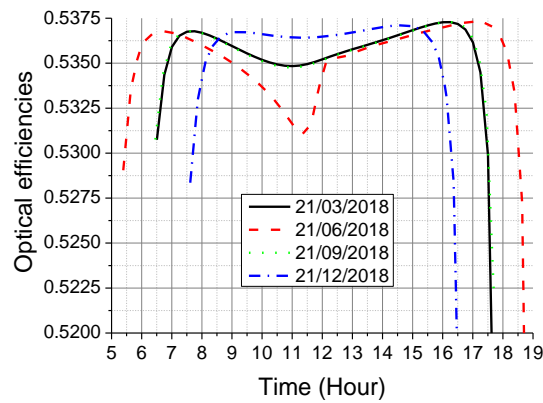


**Fig. 5.** Variation of optical efficiencies.

It is evident that the optical efficiencies variation is very reasonable from sunrise to sunset. The average values of optical efficiencies for the four days starting March through December are as follows: 0.535925, 0.5358, 0.535925 and 0.53654. It can be said that the optical efficiency of the studied device is 53.60 %; these values are very significant for this kind of solar concentrators.

As for thermal efficiency “ $\eta_{th}$ ”, it is related to the optical properties of linear Fresnel solar reflector components, related to heat loss around the absorber tube and also relates to the intercept coefficient “ $\gamma$ ”. The thermal efficiency values are always lower than the optical values. Figure (6) illustrates the thermal efficiencies evaluation according to time for the four days selected for study.

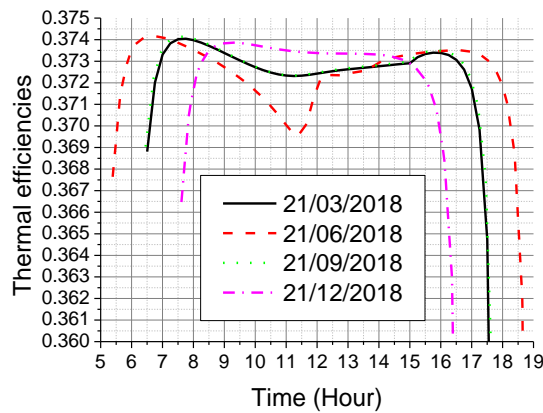


**Fig. 6.** Variation of thermal efficiencies.

It is evident that the thermal efficiencies variation is very rational from sunrise to sunset. The average values of thermal efficiencies for the four days starting March through December are as follows: 0.37275, 0.37286, 0.372835 and 0.37335. It can be said that the thermal efficiency of the studied LFR solar collector is 37.30 %; these values are substantial for this kind of solar concentrators.

### 3.3. Temperature estimation

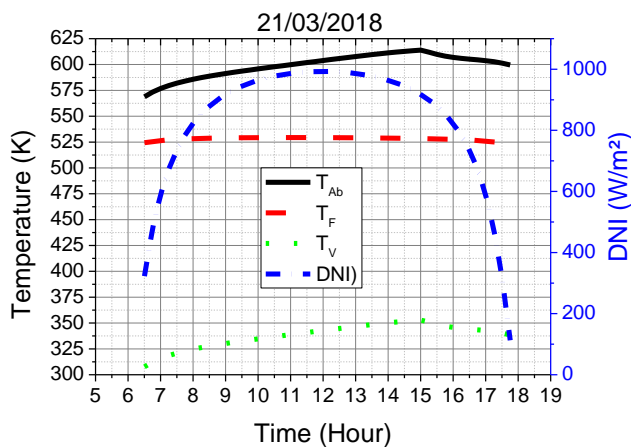
Knowing that the average mass flow of steam inside the absorber tube is 0.045 kg/s. The change in the temperature gradient between the absorber tube, the heat transfer fluid and the glass tube is directly affected by the weather conditions for each month.

Each of the next four figures (from 7 to 10) contains four curves. These curves are: the curve of the absorber tube temperature, the curve of the heat transfer tube temperature at the exit of the absorber tube, the curve of the glass tube temperature, and the fourth curve shows the change in direct solar radiation. The four curves change in terms of time.

Figure (7) shows the change in the temperatures (“TA, (K)”, “TF, (K)” and “TV, (K)”) and direct solar radiation “DNI, (W/m<sup>2</sup>)” on 21/03/2018 in terms of change in time.

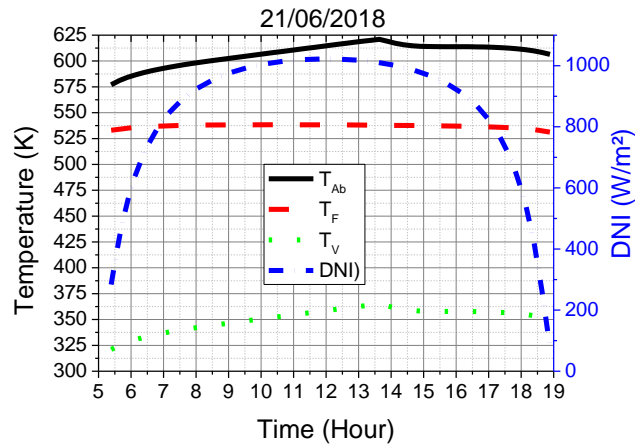
For all months, the descending order of the temperatures is as follows “TA, (K)”, “TF, (K)” and finally “TV, (K)”. It is obvious to show that the variation of the temperatures depends particularly on the incident solar power and the surrounding climatic conditions.

Table (3) contains a comparison of the results obtained by this study in terms of the days chosen to perform this numerical simulation.



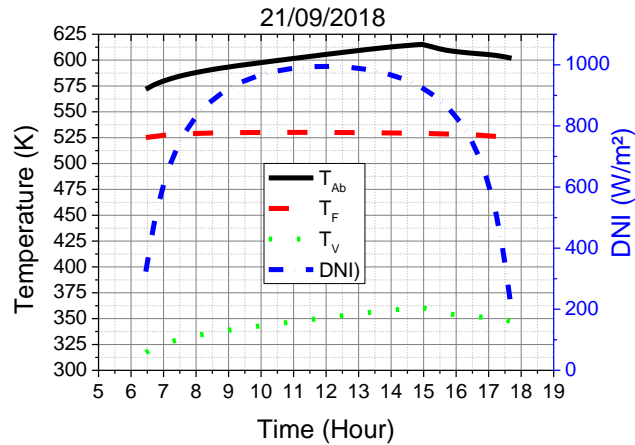
**Fig. 7.** Variation of temperatures for the day 21/03/2018.

Figure (8) shows the change in the temperatures (“TA, (K)”, “TF, (K)” and “TV, (K)”) and direct solar radiation “DNI, (W/m<sup>2</sup>)” on 21/06/2018 in terms of change in time.



**Fig. 8.** Variation of temperatures for the day 21/06/2018.

Figure (9) shows the change in the temperatures (“ $T_A$ , (K)”, “ $T_F$ , (K)” and “ $T_V$ , (K)”) and direct solar radiation “DNI, ( $W/m^2$ )” on 21/09/2018 in terms of change in time.



**Fig. 9.** Variation of temperatures for the day 21/09/2018.

Figure (10) shows the change in the temperatures (“ $T_A$ , (K)”, “ $T_F$ , (K)” and “ $T_V$ , (K)”) and direct solar radiation “DNI, ( $W/m^2$ )” on 21/12/2018 in terms of change in time.

Figures (from 7 to 10) show that:

- The steam temperature changes from 500.9913(K) to 538.3489 (K). The steam is in a superheated phase, where it can be used in the production of electricity in power plants that use Linear Fresnel solar concentrators; these stations are called the steam power plants. This station is called a concentrating thermodynamic solar power plant; it is a power plan that concentrates the direct sun's rays by means of flat mirrors in order to heat a heat transfer fluid (HTF) that generally allows the production of electricity.

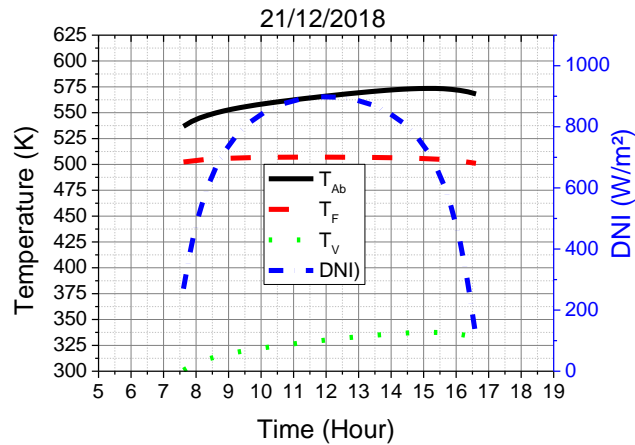


**Fig. 10.** Variation of temperatures for the day 21/12/2018.

- The absorber tube temperature changes from 536.8155 (K) to 620.9281 (K).
- The glass cover temperature varies from 300.9047 (K) to 364.8831 (K). The glass cover is transparent to sunlight but opaque to the infrared rays of the interior, which traps the heat.

### 3.4. Overall coefficient of heat loss

The absorber tube is the seat of thermal losses. Generally, the vacuum between the absorber tube and the glass tube improves the insulation against convection losses. In addition, the lower value of the absorber tube emissivity generates an increase in the thermal efficiency of the solar concentrator. Thermal loss is known as a very important parameter called the overall coefficient of heat loss “ $U_L$ , (W/m<sup>2</sup>.K)”. The thermal losses depending on the thermal insulation properties of the solar concentrator. Figure (11) shows the change in the overall coefficient of heat loss “ $U_L$ , (W/m<sup>2</sup>.K)”.

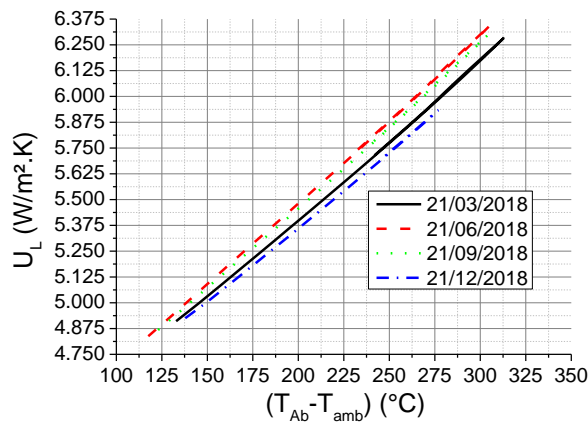


**Fig. 11.** Variation of the overall coefficient of heat loss.

The average values of overall coefficient of heat loss “ $U_L$ , (W/m<sup>2</sup>.K)” for the four days starting March through December are as follows: 5.885825 (W/m<sup>2</sup>.K), 5.98112 (W/m<sup>2</sup>.K), 5.89214 (W/m<sup>2</sup>.K) and 5.71837 (W/m<sup>2</sup>.K). For reference only, the use of a glass tube around the copper absorbent tube can reduce the overall heat loss coefficient, where it can be said that the results obtained are very acceptable.

Table (3) gives a comprehensive summary of the results obtained through this study.

**Table 3.** Comparison of LFR Solar Reflector Efficiencies.

	21/03/2018		21/06/2018		21/09/2018		21/12/2018	
	Max	Min	Max	Min	Max	Min	Max	Min
$T_{Ab}$ (K)	613.8991	568.7965	620.9281	577.038	615.2358	571.7795	573.5158	536.8155
$T_F$ (K)	529.3619	522.6609	538.3489	531.2856	530.0993	523.9656	507.0684	500.9913
$T_v$ (K)	352.8209	307.7183	364.8831	320.993	360.723	317.2666	337.605	300.9047
$U_L$ (W/m <sup>2</sup> .K)	6.28207	4.91044	6.3482	4.83799	6.29756	4.86775	5.95219	4.92507
$\eta_{opt}$	0.53728	0.50902	0.53731	0.49813	0.5373	0.52195	0.53711	0.5084
$\eta_{th}$	0.37404	0.33979	0.37417	0.32594	0.37414	0.35601	0.37387	0.33891

The results obtained are very logical, as they are controlled by seasonal climatic conditions for each of the days chosen for this study.

#### 4. Conclusion

Linear Fresnel solar thermal concentrators are devices designed to collect solar energy transmitted by direct solar radiation and communicate it to a heat transfer fluid in the form of heat. This heat energy can then be used for the production of electricity or in various industrial processes.

The optical efficiency of the device was estimated at 53.60%, where the thermal efficiency is equal to 37.30 %. As for the average values of overall coefficient of heat loss “ $U_L$ , (W/m<sup>2</sup>.K)” was limited between 5.71837 (W/m<sup>2</sup>.K) and 5.98112 (W/m<sup>2</sup>.K).

With regard to steam, the temperature in December reached 500.9913 (K). This is the lowest value recorded during the study. It is noted that the steam has exceeded the saturation phase, as it entered the superheated phase. The direct use of this superheated steam can produce electricity. This result is very encouraging to start with such investments.

The results obtained indicate that investment in this technology for the electricity production is very successful.

## References

- [1] M. Ghodbane, "Étude et optimisation des performances d'une machine de climatisation à éjecteur reliée à un concentrateur solaire " Doctorat en système énergétiques et thermiques, Département de Mécanique Université Saad Dahleb de Blida 1 2017.
- [2] M. Ghodbane, B. Boumeddane, Z. Said, and E. Bellos, "A numerical simulation of a linear Fresnel solar reflector directed to produce steam for the power plant," *Journal of Cleaner Production*, vol. 231, pp. 494-508. <https://doi.org/10.1016/j.jclepro.2019.05.201>, 2019.
- [3] M. Ghodbane, Z. Said, A. A. Hachicha, and B. Boumeddane, "Performance assessment of linear Fresnel solar reflector using MWCNTs/DW nanofluids," *Renewable Energy*, p. <https://doi.org/10.1016/j.renene.2019.10.137>, 2019.
- [4] Z. Said, M. Ghodbane, A. A. Hachicha, and B. Boumeddane, "Optical performance assessment of a small experimental prototype of linear Fresnel reflector," *Case Studies in Thermal Engineering*, doi: <https://doi.org/10.1016/j.csite.2019.100541>, 2019.
- [5] S. A. Kalogirou, "Solar thermal collectors and applications," *Progress in Energy and Combustion Science*, vol. 30, no. 3, pp. 231-295. <https://doi.org/10.1016/j.pecs.2004.02.001>, 2004.
- [6] M. Ghodbane and B. Boumeddane, "A numerical and empirical evaluation of the thermal performances of solar water heating system," presented at the International Conference on Technological Advances in Electrical Engineering (ICTAEE'16), Skikda University, October 2016.
- [7] M. Ghodbane and B. Boumeddane, "Estimating solar radiation according to semi empirical approach of PERRIN DE BRICHAMBAUT: application on several areas with different climate in Algeria," *International Journal of Energetica*, vol. 1, no. 1, pp. 20-29. <https://www.ijeca.info/index.php/IJECA/article/view/12>, 2016.
- [8] M. Ghodbane, B. Boumeddane, and N. Said, "Design and experimental study of a solar system for heating water utilizing a linear fresnel reflector," *Journal of Fundamental and Applied Sciences*, vol. 8, no. 3, pp. 804-825, <http://dx.doi.org/10.4314/jfas.v8i3.8>, 2016.
- [9] B. nature. (2018). *Les centrales à capteurs linéaires de Fresnel*, Web page: <http://3.bp.blogspot.com/-CCAzBW8D5us/VivJN8cVdMI/AAAAAAAAADX4/uF0KvqHv44/s1600/3.JPG>.
- [10] M. Ghodbane, B. Boumeddane and S. Largot, "Etude optique et thermique d'un concentrateur cylindro-parabolique en site d'Alger, Algerie," in *IXth International Congress on Renewable Energy and the Environment*, Djerba, Tunisie, 18-20 March 2015.
- [11] M. Ghodbane and B. Boumeddane, "Numerical modeling of a parabolic trough solar collector at Bouzaréah, Algeria," *International Journal of Chemical and Petroleum Sciences*, vol. 4, no. 2, pp. 11-25, 2015.
- [12] M. Ghodbane and B. boumeddane, "A numerical analysis of the energy behavior of a parabolic trough concentrator," *Journal of Fundamental and Applied Sciences*, vol. 8, no. 3, pp. 671-691, 2016 2016.
- [13] S. Bonnet, M. Alphilippe, and P. Stouffs, "Conversion thermodynamique de l'énergie solaire dans des installations de faible ou de moyenne puissance: Réflexion sur choix du meilleurs degré de concentration," in *Revue d'énergie renouvelable: 11 ème journée internationales de thermique*, 2003, pp. 73-80.

- [14] D. G. Yogi, F. Kreith, and J. F. Kreider, "Off-Normal Incidence Effects," in *Principles of solar engineering*, T. Francis., Ed. 2nd Edition ed., 1999, p. 139.
- [15] J. A. Duffie and W. A. Beckman, *Solar Engineering of Thermal Processes*, 4th ed. Wiley, 2013.
- [16] L. Marletta and G. Evola, "thermodynamic analysis of a hybrid photovoltaic/thermal solar collector," *international journal of heat and technology*, vol. 31, no. 2, pp. 135-142, 2013. DOI: 10.18280/ijht.310218.

**ECHAHID HAMMA LAKHDAR UNIVERSITY - EL-OUED**  
**Under the Supervision of the DGRSDT and in collaboration with the CRTI**  
**International Pluridisciplinary PhD Meeting (IPPM'20)**  
**23-26, 2020 1<sup>st</sup> Edition, February**  
**Theme: Renewable Energy**